Technetium Metallothionein: Spectroscopic and EXAFS Study of $^{99}TcO^{3+}$ Binding to Zn_7-Metallothionein

William B. Jones,[†] Timothy E. Elgren,[‡] Maurice M. Morelock,[§] R. C. Elder,*[,†] and Dean E. Wilcox*[,‡]

Department of Chemistry, University of Cincinnati, Cincinnati, Ohio 45221-0172, Department of Chemistry, Dartmouth College, Hanover, New Hampshire 03755-3564, and Immunopharmaceutical Research Division, Medical Products Department, E. I. DuPont de Nemours & Company, 331 Treble Cove Road, North Billerica, Massachusetts 01862

Received May 4, 1994[⊗]

Vibrational, absorption, circular dichroism, and Tc K-edge extended X-ray absorption fine structure (EXAFS) measurements have been made on three samples of metallothionein (MT) containing 1.6, 3.9, and 6.2 mol equiv of ^{99}Tc, prepared by the metal displacement (transchelation) reaction of $TcO(glucoheptonate)_2^-$ with Zn_7-MT. For all three samples the TcO^{3+} ion is bound to the protein in a square pyramidal coordination with equatorial ligands consisting of ~2 cysteine thiolates and, surprisingly, ~2 O/N donor ligands. As the Tc content increases, there is very little change in the Tc coordination, except for a decrease in the number of cysteine ligands per TcO^{3+} for $Tc_{6.2}$-MT. The unusual ligand set for this metal ion when it is bound to MT, the absence of bridging cysteine ligands, and the significant number of cysteines not involved in binding TcO^{3+}, indicate that transchelation does not involve a simple substitution of TcO^{3+} for Zn(II).

Introduction

Technetium-99m has properties which make it ideal for diagnostic radioimaging: it emits a 140 keV γ ray with energy sufficient to escape organs located deep in the body, it has a 6 h half-life, and it can be generated readily in clinical settings.[1] Already the imaging isotope of choice, recent research has focused on developing new Tc compounds with improved organ specificity. The immune system, however, achieves exquisite biospecificity and there is considerable potential for using antibodies as carriers for radioimaging and radiotherapeutic isotopes.[2] This can be accomplished by binding radioisotopes directly to the antibody protein[2b] or by using a bifunctional metal carrier attached to the antibody.[2c] The latter has certain advantages including metal binding site(s) which can be tailored to provide stable, inert chelation of the desired metal and minimize nonspecific, labile binding of the metal to the antibody. Due to its high affinity for certain metal ions, the small protein metallothionein has the potential to be used as such a bifunctional carrier for radioisotopes, such as ^{99m}Tc.[3]

Metallothioneins (MT) are a class of small proteins that have a high cysteine (Cys) content (~30%) and homology, exhibit a high affinity for both toxic (Cd(II), Hg(II), etc.) and essential (Cu(I), Zn(II)) metals *in vivo*, typically bind 7 mol equiv of dipositive metal ions, and are synthesized in response to metal ion exposure.[4] Based on these properties, MT is generally thought to play a role in metal detoxification and homeostasis. As indicated by ^{113}Cd NMR[5] and proteolysis[6] studies, the 61 residue mammalian MT consists of two peptide domains which bind metals independently. Detailed structures of Cd_7-MT and native (Cd_5Zn_2)-MT have been obtained from NMR[7] and X-ray crystallography[8] studies, respectively: the N-terminal β domain, which contains 9 Cys, binds 3 Cd(II) (2 Zn(II) and 1 Cd(II) in native) in tetrahedral (T_d) tetrathiolate coordination with bridging and terminal Cys ligands; the C-terminal α domain, which contains 11 Cys, binds 4 Cd(II) in similar T_d tetrathiolate coordination with bridging and terminal Cys. Monopositive metals bind with different stoichiometry (typically 12 mol equiv) and thiolate coordination; extended X-ray absorption fine structure (EXAFS) studies have indicated two-coordinate Au(I)[9] and three-coordinate Cu(I)[10] bound to MT. In addition, Pt-

[†] University of Cincinnati.
[‡] Dartmouth College.
[§] DuPont. Current address: Research and Development Center, Boehringer-Ingleheim Pharmaceuticals, 900 Ridgebury Rd., Ridgefield, CT 06877-0368.

[⊗] Abstract published in *Advance ACS Abstracts,* November 1, 1994.

(1) (a) Deutsch, E.; Libson, K.; Jurisson, S.; Lindoy, L. F. *Prog. Inorg. Chem.* **1983**, *30*, 75−139. (b) Clarke, M. J.; Fackler, P. H. *Struct. Bonding* **1982**, *50*, 57−78. (c) Pinkerton, T. C.; Desilets, C. P.; Hoch, D. J.; Mikelsons, M. V.; Wilson, G. M. *J. Chem. Educ.* **1985**, *62*, 965−973. (d) Clarke, M. J.; Podbielski, L. *Coord. Chem. Rev.* **1987**, *78*, 253−331.

(2) (a) Hnatowich, D. J. *Nucl. Med. Biol.* **1990**, *17*, 49−55. (b) Rhodes, B. A. *Nucl. Med. Biol.* **1991**, *18*, 667−676. (c) Meares, C. F. *Nucl. Med. Biol.* **1986**, *13*, 311−318.

(3) (a) Brown, B. A.; Drozynski, C. A.; Dearborn, C. B.; Hadjian, R. A.; Liberatore, F. A.; Tulip, T. H.; Tolman, G. L.; Haber, S. B. *Anal. Biochem.* **1988**, *172*, 22−28. (b) Tolman, G. L. Trace-Labeled Conjugates of Metallothionein and Target Seeking Biologically Active Molecules. U.S. Patent 4,732,864, 1988.

(4) (a) Kägi, J. H. R., Nordberg, M., Eds. *Metallothionein*; Birkhäuser Verlag: Basel, 1979. (b) Kägi, J. H. R.; Kojima, Y., Eds. *Metallothionein II*; Birkhäuser Verlag: Basel, 1987. (c) Kägi, J. H. R.; Schäffer, A. *Biochemistry* **1988**, *27*, 8509−8515. (d) Stillman, M. J., Shaw, C. F., III, Suzuki, K. T., Eds. *Metallothioneins*; VCH: New York, 1992.

(5) Otvos, J. D.; Armitage, I. M. *Proc. Natl. Acad. Sci. U.S.A.* **1980**, *77*, 7094−7098.

(6) (a) Winge, D. R.; Miklossy, K.-A. *J. Biol. Chem.* **1982**, *257*, 3471−3476. (b) Nielson, K. B.; Winge, D. R. *J. Biol. Chem.* **1984**, *259*, 4941−4946.

(7) Frey, M. H.; Wagner, G.; Vasák, M.; Sørensen, O. W.; Neuhaus, D.; Wörgötter, E.; Kägi, J. H. R.; Ernst, R. R.; Wüthrich, K. *J. Am. Chem. Soc.* **1985**, *107*, 6847−6851.

(8) Robbins, A. H.; McRee, D. E.; Williamson, M.; Collett, S. A.; Xuong, N. H.; Furey, W. F.; Wang, B. C.; Stout, C. D. *J. Mol. Biol.* **1991**, *221*, 1269−1293.

(9) Laib, J. E.; Shaw, C. F., III; Petering, D. H.; Eidness, M. K.; Elder, R. C.; Garvey, J. S. *Biochemistry* **1985**, *24*, 1977−1986.

(10) (a) George, G. N.; Winge, D.; Stout, C. D.; Cramer, S. P. *J. Inorg. Biochem.* **1986**, *27*, 213−220. (b) Smith, T. A.; Lerch, K.; Hodgson, K. O. *Inorg. Chem.* **1986**, *25*, 4677−4680. (c) George, G. N.; Byrd, J.; Winge, D. *J. Biol. Chem.* **1988**, *263*, 8199−8203.

0020-1669/94/1333-5571$04.50/0

(II) binding to MT has been studied and square planar tetrathiolate coordination has been suggested.[11]

Previously it was shown that both the metastable isotope ^{99m}Tc and its long-lived ground state ^{99}Tc ($t_{1/2} = 2.12 \times 10^5$ years), introduced with the complex $TcO(GH)_2^-$ (GH = glucoheptonate(2−)), bind to Zn_7-MT presumably by transchelation (metal ion displacement).[12] The resulting Tc,Zn-MT exhibits (1) a 405 nm absorption band (ϵ per Tc $\approx$ 2500 M^{-1} cm^{-1}), assigned as a thiolate-to-Tc(V) charge transfer (CT) transition, (2) a ~570 nm absorption shoulder, assigned as a Tc(V) ligand field band, and (3) a strong Raman band in the 940−960 cm^{-1} region, assigned as the Tc=O stretching mode of a tightly bound oxo ligand. TcO^{3+} binding is rapid enough for radiopharmaceutical applications (>75% Tc binding to 10^{-5} M Zn_7-MT in 30 min at pH 6.5) and approaches a maximum stoichiometry of 7 mol equiv of bound Tc; further, TcO^{3+} binds with very high affinity, as it is not displaced from the protein at pH 1. All of these properties make MT an important candidate for ^{99m}Tc chelation in nuclear medicine applications.[3]

However, the structural properties of Tc,Zn-MT are poorly understood, as is the transchelation process. While there is a linear increase in the 405 nm Cys-to-Tc(V) CT intensity with increasing mole equivalents of Tc bound to MT, other data suggest that no additional Cys thiolates are involved in binding the fourth, fifth, and even sixth mol equiv of Tc.[12] This could be due to TcO^{3+} binding to only one domain or to the inaccessibility of certain thiolates as transchelation proceeds; protein ligands other than Cys may also be involved in binding Tc. The substitution of TcO^{3+} for Zn(II) is of further interest because it involves replacement of a dipositive metal found predominantly in T_d coordination by a high oxidation state metal typically found in square pyramidal complexes.

In this study, we have used vibrational, optical and EXAFS methods to characterize the properties of three ^{99}Tc,Zn-MT samples, prepared by the reaction of $TcO(GH)_2^-$ with Zn_7-MT and containing 1.6, 3.9 and 6.3 mol equiv of Tc. At all Tc stoichiometries a square pyramidal $TcO(Cys)_{2\pm1}$(O/N donor ligand)$_{2\pm1}$ coordination is found for TcO^{3+} bound to the protein, establishing this as one of the few examples of a metal ion bound to MT without homoleptic Cys (thiolate) ligation. These data also provide additional insight into the process of transchelation binding of TcO^{3+} to Zn_7-MT.

Experimental Section

Caution! Technetium-99 is a weak β emitter with a half-life of 2.12×10^5 years and an average particle energy of 85 keV. All manipulations were carried out in laboratories approved for radioisotope use and standard precautions and practices for working with weak β emitting isotopes were followed.

Samples. Rabbit liver metallothionein-1 was isolated and purified, Zn_7-MT samples were obtained by metal reconstitution, and three $^{99}Tc_x$-MT samples were prepared by dialysis of Zn_7-MT against 2, 5 and 20 mol equiv of $^{99}TcO(GH)_2^-$, as described previously.[12] The reactions were stopped after 4 h by exhaustive dialysis against metal free water and the samples were lyophilized. ^{99}Tc incorporation was quantified by liquid scintillation counting, which showed that the three protein samples contained 1.6, 3.9 and 6.2 mol equiv ^{99}Tc, respectively.

Technetium model compounds used in the X-ray absorption studies included $NaTcO_4$, obtained from NEN-DuPont, and $NaTcO(edt)_2$ (edt = ethane-1,2-dithiolate(2−))[13] and $(TcO)_2(edt)_3$,[14] generously supplied by Professor Alan Davison of MIT.

Spectroscopic Measurements. For spectroscopic studies, the lyophilized protein samples were dissolved in distilled, deionized water that had been passed through an additional column of Chelex 100 (Bio-Rad) and deoxygenated prior to use. Aliquots of each sample were diluted in 10 mL of Aquasol (NEN-DuPont) in glass scintillation vials for liquid scintillation determination of the ^{99}Tc concentration. The protein concentrations were then determined to be 1.4×10^{-4} M for $Tc_{1.6}$-MT, 1.9×10^{-4} M for $Tc_{3.9}$-MT, and 1.6×10^{-4} M for $Tc_{6.2}$-MT, based on the mol equiv of ^{99}Tc in each sample.

Circular dichroism (CD) spectra were recorded at room temperature on an Instruments SA Mark V dichrograph calibrated with standard solutions of (*S*)-10-camphorsulfonic acid and nickel(II) tartrate.[15] Absorption spectra were recorded at room temperature on a Hewlett Packard 8451A diode array spectrophotometer using a 1.0 cm quartz cuvette. Raman measurements were obtained at room temperature with a Coherent INNOVA-18 argon ion laser and a Spex Ramalog system operating with 90° scattering, 4 cm^{-1} bandpass, and 5 s response time. Raman frequencies were calibrated with the 2249 cm^{-1} band of neat CH_3CN. Samples were placed in glass capillary tubes and excited with ~30 mW power (measured at the sample) at 457.9 nm. Resonance enhancement was measured with other Ar^+ laser lines (similar power at the sample) and determined relative to the 975 cm^{-1} band of a SO_4^{2-} internal standard (0.10 M Na_2SO_4).

X-ray Absorption Measurements. For X-ray absorption measurements, the lyophilized protein samples and Tc model compounds were mixed with Coffeemate, pressed into 0.60 × 1.50 × 0.10 cm pellets, sealed with Kapton tape, and loaded into aluminum sample holders.

Technetium K-edge (21 047.3 eV) X-ray absorption data were collected in fluorescence mode to 16.5 $Å^{-1}$ in momentum space at wiggler station IV-3 at the Stanford Synchrotron Radiation Laboratory, as described previously.[16] Samples were held at 10 K throughout the experiment using a flowing liquid helium cryostat (Oxford Instruments CF1208). A pre-edge and three region spline was fitted to the raw data to normalize the EXAFS region. Data reduction and optimization were performed with a modified version of XFPAK (Professor Robert Scott, University of Georgia).[17]

Results and Analysis

UV−Visible Absorption, Circular Dichroism, and Vibrational Measurements. As in the initial report of Tc,Zn-MT,[12] the three metallothionein samples studied here, which have 1.6, 3.9 and 6.2 mol equiv of ^{99}Tc, all exhibit absorption bands at 405 and ~570 (shoulder) nm (Figure 1). The former band has been assigned as a thiolate-to-Tc(V) CT transition, by comparison to spectra of structurally characterized Tc(V) thiolate complexes,[13,14,18] and confirms Cys ligation. However, while the *absorbance* at 405 nm increases constantly with increasing Tc content up to ~6 mol equiv, the tail of a higher energy band adds to this intensity (indicated by the disappearance of the minimum at 350 nm) and the *integrated intensity* (obtained

(11) (a) Bongers, J.; Bell, J. U.; Richardson, D. E. *J. Inorg. Biochem.* **1988**, *34*, 55−62. (b) Bongers, J.; Bell, J. U.; Richardson, D. E. *Inorg. Chem.* **1991**, *30*, 515−519. (c) Pattanaik, A.; Bachowski, G.; Laib, J.; Lemkuil, D.; Shaw, C. F., III; Petering, D. H.; Hitchcock, A.; Saryan, L. *J. Biol. Chem.* **1992**, *267*, 16121−16128.

(12) Morelock, M. M.; Cormier, T. A.; Tolman, G. L. *Inorg. Chem.* **1988**, *27*, 3137−3140.

(13) (a) Smith, J. E.; Byrne, E. F.; Cotton, F. A.; Sekutowski, J. C. *J. Am. Chem. Soc.* **1978**, *100*, 5571−5572. (b) Smith, J. E.; Byrne, E. F. *Inorg. Chem.* **1979**, *18*, 1832−1835.

(14) (a) DePamphilis, B. V.; Jones, A. G.; Davison, A. *Inorg. Chem.* **1983**, *22*, 2292−2297. (b) Davison, A.; DePamphilis, B. V.; Faggiani, R.; Jones, A. G.; Lock, C. J. L.; Orvig, C. *Can. J. Chem.* **1985**, *19*, 1988−1992.

(15) Konno, T.; Meguro, H.; Murakami, T.; Hatano, M. *Chem. Lett.* **1981**, 953.

(16) (a) Martin, J. L., Jr.; Yuan, J.; Lunte, C. E.; Elder, R. C.; Heineman, W. R.; Deutsch, E. *Inorg. Chem.* **1989**, *28*, 2899−2901. (b) Elder, R. C.; Eidsness, M. K. *Chem. Rev.* **1987**, *87*, 1027−1046.

(17) Scott, R. A. *Methods Enzymol.* **1985**, *117*, 414−459.

(18) (a) DePamphilis, B. V.; Jones, A. G.; Davis, M. A.; Davison, A. *J. Am. Chem. Soc.* **1978**, *100*, 5570−5571. (b) Davison, A.; Orvig, C.; Trop, H. S.; Sohn, M.; DePamphilis, B. V.; Jones, A. G. *Inorg. Chem.* **1980**, *19*, 1988−1992.

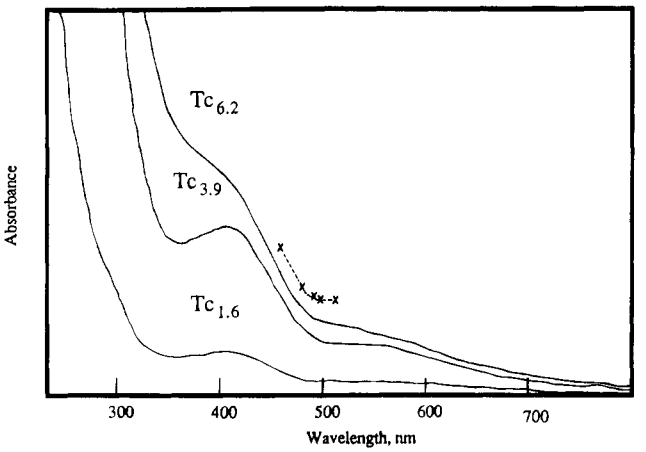

Figure 1. Near-UV and visible absorption spectra of unbuffered aqueous solutions of three Tc_x-MT (x = 1.6, 3.9, 6.2) samples. Relative intensity of the 940 cm^{-1} Raman band of the $Tc_{3.9}$-MT sample with laser exitation at 457.9, 488.0, 496.5, 501.7 and 514.5 nm is indicated (×).

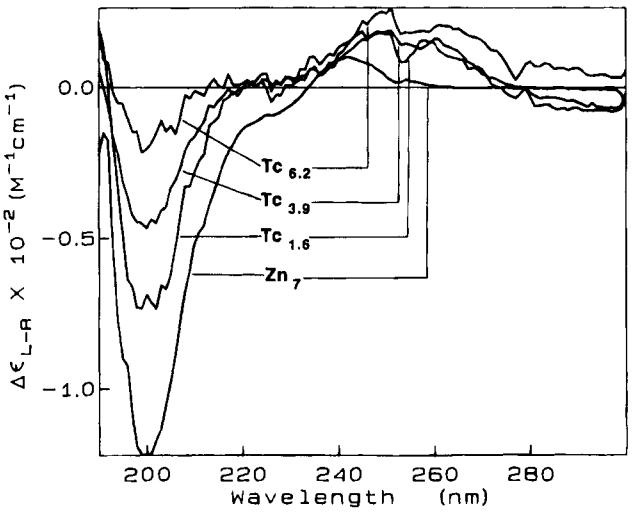

Figure 2. UV CD spectra of unbuffered aqueous solutions of Zn_7-MT and three Tc_x-MT (x = 1.6, 3.9, 6.2) samples.

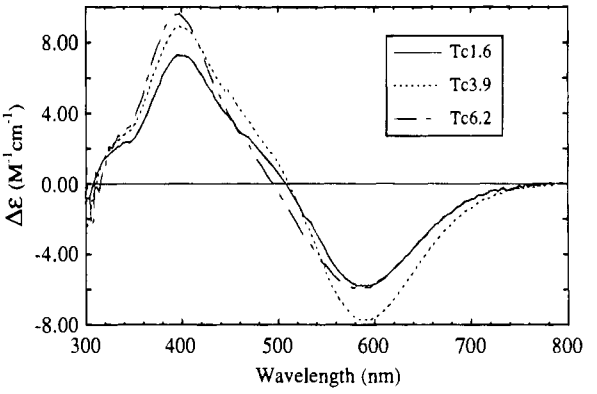

Figure 3. Near-UV and visible CD spectra of unbuffered aqueous solutions of three Tc_x-MT (x = 1.6, 3.9, 6.2) samples.

through band shape analysis) of the 405 nm thiolate-to-Tc(V) CT band does not increase beyond 4 mol equiv of Tc.[19]

These samples, as reported previously,[12] have an intense Raman band at 940 cm^{-1} (data not shown), assigned as the Tc=O stretching mode. It is found at the same energy for all three samples and increases in intensity with increasing Tc content of the protein (relative integrated intensity: $Tc_{1.6}$, 7; $Tc_{3.9}$, 18; $Tc_{6.2}$, 41).[20] Thus, the TcO^{3+} ion binds to MT at all stoichiometries, and the Tc=O vibrational frequency is consistent with that of five-coordinate square pyramidal or possibly six-coordinate[21] TcO^{3+} complexes.[13,14,18,22] This vibrational band broadens somewhat with increasing Tc stoichiometry (fwhm: $Tc_{1.6}$, 31 cm^{-1}; $Tc_{3.9}$, 33 cm^{-1}; $Tc_{6.2}$, 39 cm^{-1}), suggesting only a modest increase in heterogeneity of the TcO^{3+} coordination. An excitation profile for the $Tc_{3.9}$ sample (Figure 1) shows preresonance enhancement of this vibrational mode by excitation at higher energy, indicating resonance enhancement from the absorption band at 405 nm or one at higher energy.

The 190−240 nm region of the CD spectrum can be useful for monitoring changes in the secondary structure of proteins. The UV CD spectrum of Zn_7-MT (Figure 2) shows a strong negative band at 200 nm and a weak positive band at 240 nm, as reported previously.[23] Negative CD intensity in the 190−200 nm region is associated with random secondary structure,[24] consistent with MT structures determined by NMR[7] and X-ray crystallography,[8] which show only the presence of several β turns. An identical negative 200 nm CD band is also found for Cd_7-MT and apo (metal-free) MT,[23] indicating a similar absence of secondary structure. As the Tc content of MT increases from 1.6 to 6.2 mol equiv, the 200 nm CD band shows a steady decrease in its negative intensity (Figure 2). While this could be interpreted as a decrease in the amount of random secondary structure, relative to Zn_7-MT, Cd_7-MT and apo MT, CD bands characteristic of α helix or β sheet ((+)190−193 nm and (−)220−222 nm)[24] do not develop. Alternatively, when TcO^{3+} is bound in the chiral environment provided by the protein, CT or Rydberg transitions of the open shell Tc(V) ion may contribute positive 200 nm CD intensity, which increases with Tc stoichiometry and cancels the negative 200 nm CD band of the peptide. Thus, in contrast to Zn(II) and Cd(II), when open shell metal ions bind to proteins at high metal-to-residue ratios, UV CD spectral data are unreliable for determining protein secondary structure; this appears to be the case here.

The UV and visible CD spectra of the Tc_x-MT samples show three prominent features associated with Tc binding: a broad positive band in the 240−270 nm region (Figure 2), a positive band at 400 nm and a negative band at 595 nm (Figure 3). No isosbestic points are observed as the Tc content is increased and, in particular, the 450−550 nm region is complex. Further, the CD bands do not show steady changes in intensity with increasing Tc content, paralleling the behavior of the integrated intensity of the 405 nm absorption band (Figure 1). In particular, the 595 nm negative CD band actually decreases in intensity and shifts slightly to higher energy with >4 mol equiv of Tc.

To provide additional insight about Tc binding to MT and allow a simple ligand field analysis of TcO^{3+} coordination, the near-UV and visible CD spectra (Figure 3) were transformed to an energy scale and subjected to band shape analysis. The best fit of Gaussian bands to the CD spectrum of the $Tc_{3.9}$-MT sample is shown in Figure 4 and the peak energies and intensities

(19) A plot of the integrated intensity of the previously reported[12] 405 nm absorption band versus bound Tc shows a steady increase up to 4 mol equiv of Tc but smaller increases for higher Tc stoichiometries.
(20) Because of the possibility of resonance enhancement of this vibration at higher Tc stoichiometries (higher optical densities at 457.9 nm), it is not possible to relate intensity of this band to the concentration of TcO^{3+} ions in the sample.
(21) The energy of the Tc=O vibrational band does not allow us to distinguish the presence or absence of a sixth ligand *trans* to the oxo.
(22) (a) Bandoli, G.; Mazzi, U.; Roncari, E.; Deutsch, E. *Coord. Chem. Rev.* **1982**, *44*, 191−227. (b) Melnik, M.; Van Lier, J. E. *Coord. Chem. Rev.* **1987**, *77*, 275−324.
(23) Pande, J.; Pande, C.; Gilg, D.; Vasák, M.; Callender, R.; Kägi, J. H. R. *Biochemistry* **1986**, *25*, 5526−5532.
(24) Johnson, W. C., Jr. *Methods Biochem. Anal.* **1984**, *31*, 61−163.

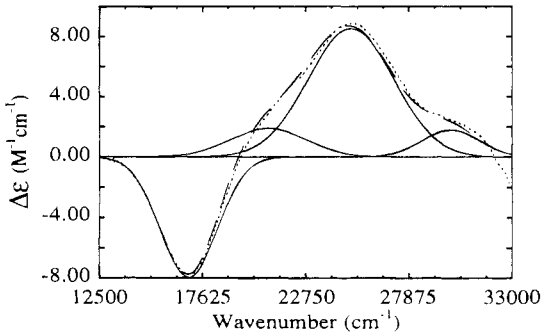

Figure 4. Gaussian band shape analysis of the near-UV and visible CD spectrum of the $Tc_{3.9}$-MT sample: (•••) experimental spectrum, (—) Gaussian bands, (— —) sum of Gaussian bands. See Table 1 for fit parameters.

Table 1. Gaussian Band Shape Analysis of Tc_x-Metallothionein CD Spectra

sample	band position, cm^{-1} ($\Delta\epsilon$, M^{-1} cm^{-1})[a]	band position, nm
$Tc_{1.6}$-MT	16 922 (−5.73)	591
	20 600 (0.9)	485
	24 860 (7.15)	402
	30 000 (1.55)	333
$Tc_{3.9}$-MT	16 950 (−7.95)	590
	20 912 (1.9)	478
	25 000 (8.55)	400
	29 955 (1.8)	334
$Tc_{6.2}$-MT	17 075 (−5.85)	586
	21 400 (0.4)	467
	25 147 (9.3)	398
	29 900 (1.5)	334

[a] $\Delta\epsilon$ values are those required to reproduce the original CD spectra and are based on protein concentrations.

obtained for all three Tc_x-MT samples are indicated in Table 1. Band shape analysis shows that fitting the 800−300 nm (12 500−33 000 cm^{-1}) CD spectrum requires a minimum of four Gaussian bands, including a weak positive band in the 450−500 nm region. For the $Tc_{3.9}$-MT sample these are found at (−)590 nm (16 950 cm^{-1}), (+)478 nm (20 912 cm^{-1}), (+)400 nm (25 000 cm^{-1}), and (+)334 nm (29 955 cm^{-1}).

Simple ligand field analysis of the TcO^{3+} electronic properties provides insight about the coordination of this ion to MT. Initially the $Tc_{1.6}$-MT sample is considered. The 940 cm^{-1} Tc=O stretching frequency, the 405 nm thiolate-to-Tc(V) CT absorption band (402 nm CD band), and the ~570 nm ligand field absorption band (591 nm CD band) of this sample are all similar to analogous vibrational and spectral data of structurally characterized TcO^{3+} complexes with thiolate ligands, square pyramidal coordination, and a $^1A_1$ groundstate (d_{xy}^2 configuration).[13,14,18] A d^2 ion in effective C_{4v} symmetry has three spin-allowed ligand field transitions in the following expected order of increasing energy: $^1E\{(d_{xz},d_{yz})^1(d_{xy})^1\} \leftarrow {}^1A_1\{(d_{xy})^2\}$; $^1A_2\{(d_{x^2-y^2})^1(d_{xy})^1\} \leftarrow {}^1A_1\{(d_{xy})^2\}$; $^1B_2\{(d_{z^2})^1(d_{xy})^1\} \leftarrow {}^1A_1\{(d_{xy})^2\}$. Only the first of these is both electric- and magnetic-dipole allowed and should be the d−d transition with the highest absorption and CD intensity. The 591 nm CD band is the only feature in the 800−300 nm region with a Kuhn anisotropy factor[25] ($|\Delta\epsilon|/\epsilon = 0.0059$) large enough to be a magnetic-dipole allowed transition and this band is assigned as the $^1E \leftarrow {}^1A_1$ ligand field transition; this assignment is consistent with data for several five- and six-coordinate TcO^{3+} complexes (Table 2). The next highest energy CD band is found at 485 nm and is assigned as the $^1A_2 \leftarrow {}^1A_1$ transition. The 405 nm absorption band (402 nm CD feature), based on its intensity and similarity in energy to those of structurally characterized TcO^{3+} thiolate complexes, has been assigned as a thiolate-to-Tc(V) CT transition. The highest energy CD band at 333 nm is either the highest energy ligand field transition, $^1B_2 \leftarrow {}^1A_1$, or possibly another CT transition. Finally, the excitation profile of the Tc=O vibrational band (Figure 1) suggests that it is enhanced by excitation into a transition with $\lambda_{max} < 458$ nm. This pre-resonance enhancement of the Tc=O stretching mode could be from the 405 nm thiolate-to-Tc(V) CT transition, as observed for the Mo=O stretching mode of MoO_2(2,3:8,9-dibenzo-1,4,7,-10-tetrathiadecane).[26] Alternatively, this enhancement could be associated with the 333 nm band, particularly if it is a CT transition associated with the TcO^{3+} ion.[27]

Based on this assignment for the $Tc_{1.6}$-MT sample, the effects of increased Tc loading on the TcO^{3+} coordination to the protein are considered. Band shape analysis (Table 1) shows that the most obvious perturbation of the TcO^{3+} ligand field with higher Tc content is the shift of the $^1A_2 \leftarrow {}^1A_1$ transition to higher energy; this is the source of complexity in the 450−550 nm region (Figure 3). This d−d transition is associated with the equatorial ligand field and the 800 cm^{-1} shift of this band to higher energy reflects a perturbation of the equatorial ligands. One plausible explanation for this shift would be the change from a $\sim D_{2d}$ distorted equatorial ligand field to a more planar one; alternatively, this shift could originate from a change in the equatorial ligands.

X-ray Absorption Measurements. The EXAFS region of the X-ray absorption spectrum provides quantitative radial information about the identity, distance, and number of atoms around the absorbing element.[28] To characterize Tc coordination in these three MT samples, X-ray absorption measurements were made at the technetium K edge and the EXAFS region was analyzed.[16] Figure 5 shows the three normalized EXAFS spectra weighted by k^3; the improved signal-to-noise in the 11.5−16.5 $Å^{-1}$ region of the $Tc_{6.2}$-MT spectrum is attributed to the higher Tc content of this sample. The Fourier transforms (FT) of the three EXAFS data sets (3.0−16.5 $Å^{-1}$) provide the pseudo-radial distribution functions (PRDF) shown in Figure 6. The PRDF for each sample exhibits six peaks below 3.0 Å $R+\alpha$. The number and relative intensities of these peaks are significantly different than all reported FT-EXAFS data on MT,[9,10,11c,29,30] suggesting unique structural features of TcO^{3+} coordination to MT. These peaks, labeled A−F, are similar in location but differ in intensity from sample to sample, suggesting there is no major difference in the Tc coordination among these samples. Since these peaks, except for B and C, are resolved in all three FT data sets (Figure 6), each peak was individually back transformed into momentum space; the resulting filtered back-transformed data were then analyzed by fitting with

(25) Gillard, R. D. In *Physical Methods in Advanced Inorganic Chemistry*; Hill, H. A. O.; Day, P., Eds.; Wiley-Interscience: New York, 1968; Chapter 5.

(26) Subramanian, P.; Burgmayer, S.; Richards, S.; Szalai, V.; Spiro, T. G. *Inorg. Chem.* **1990**, *29*, 3849−3853.

(27) The $^1B_2 \leftarrow {}^1A_1$ ligand field transition results in excited state population of the d_{z^2} orbital involved in σ Tc−O bonding; however, due to the low molar extinction values of d−d transitions, only rarely are they associated with resonance enhancement of metal−ligand vibrations.

(28) (a) Cramer, S. P.; Hodgson, K. O. *Prog. Inorg. Chem.* **1979**, *25*, 1−39. (b) Eisenberger, P.; Kincaid, B. M. *Science* **1978**, *200*, 1441−1447.

(29) (a) Abrahams, I. L.; Garner, C. D.; Bremner, I.; Diakun, G. P.; Hasnain, S. S. *J. Am. Chem. Soc.* **1985**, *107*, 4596−4597. (b) Abrahams, I. L.; Bremner, I.; Diakun, G. P.; Garner, C. D.; Hasnain, S. S.; Ross, I.; Vasák, M. *Biochem. J.* **1986** *236*, 585−589. (c) Hasnain, S. S.; Diakun, G. P.; Abrahams, I. L.; Ross, I.; Garner, C. D.; Bremner, I.; Vasák, M. in ref 4b, pp 227−236.

(30) Freedman, J. H.; Powers, L.; Peisach, J. *Biochemistry* **1986**, *25*, 2342−2349.

Table 2. Electronic Absorption Features of TcO^{3+} Complexes

complex	absorption bands, nm (ϵ, M^{-1} cm^{-1})	
	5-Coordinate Complexes	
$(Bu_4N)[TcOX_4]$, in CH_2Cl_2	X = Cl[a]	X = Br[a,b]
	842 (10)	615 (22)
	635 (10)	478 (113)
	576 (10)	353 (3750)
	458 (30)	248 (10 400)
	377 (150)	
	295 (4080)	
$(Ph_4As)[TcO(ethane\text{-}1,2\text{-}dithiolate)_2]$, in CH_3CN[c]	484 (sh)	
	433 (sh)	
	399 (3400)	
	279 (7750)	
$TcO(glucoheptonate)_2^-$ [d]	502 (65)	
	275 (2800)	
	6-Coordinate Complexes	
$(NH_4)_2[TcOCl_5]$, in conc HCl[e]	935 (18) ($^1E \leftarrow {}^1A_1$)	
	600 (6) ($^1A_2 \leftarrow {}^1A_1$)	
	485 (24) ($^1B_2 \leftarrow {}^1A_1$)	
	294 (4400)	
	229 (10 600)	
$K_2TcO(CN)_5{\cdot}4H_2O$, in H_2O[f]	680 (60)	
	466 (680)	
	387 (46 900)	
$TcO(hydrotris(1\text{-}pyrazolyl)borato)X_2$, in CH_2Cl_2	X = Cl[g]	X = Br[b]
	792 (78)	784 (80)
	375 (sh)	311 (5600)
	33 (5900)	

[a] Preetz, M.; Peters, G. *Z. Naturforsch.* **1980**, *35B*, 1355–1358. [b] Thomas, R. W.; Davison, A.; Trop, H. S.; Deutsch, E. *Inorg. Chem.* **1980**, *19*, 2840–2842. [c] Reference 18b. [d] Reference 33. [e] Jezowska-Trzebiatowska, B.; Wajda, S.; Baluka, M. *Zh. Strukt. Khim.* **1967**, *8*, 519–523. [f] Trop, H. S.; Jones, A. G.; Davison, A. *Inorg. Chem.* **1980**, *19*, 1993–1997. [g] Thomas, R. W.; Estes, G. W.; Elder, R. C.; Deutsch, E. *J. Am. Chem. Soc.* **1979**, *101*, 4581–4585.

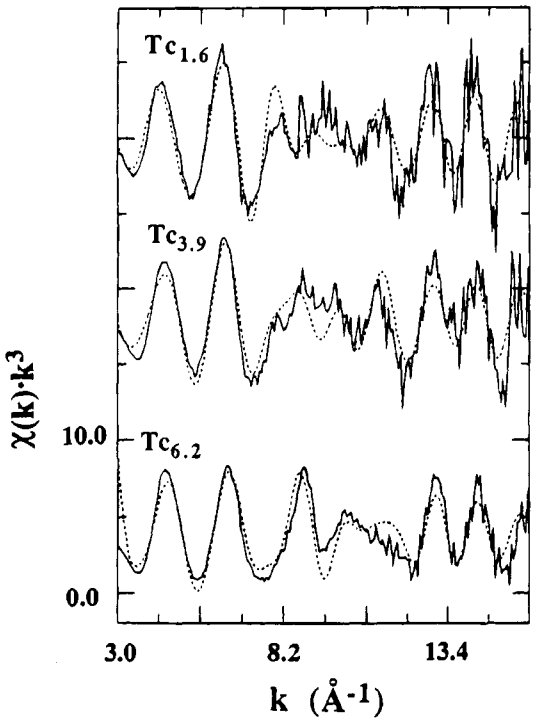

Figure 5. Normalized Tc K-edge EXAFS spectra, weighted by k^3 (—), and EXAFS spectra calculated with the best fit parameters (see Table 3) (•••) for three Tc_x-MT (x = 1.6, 3.9, 6.2) samples.

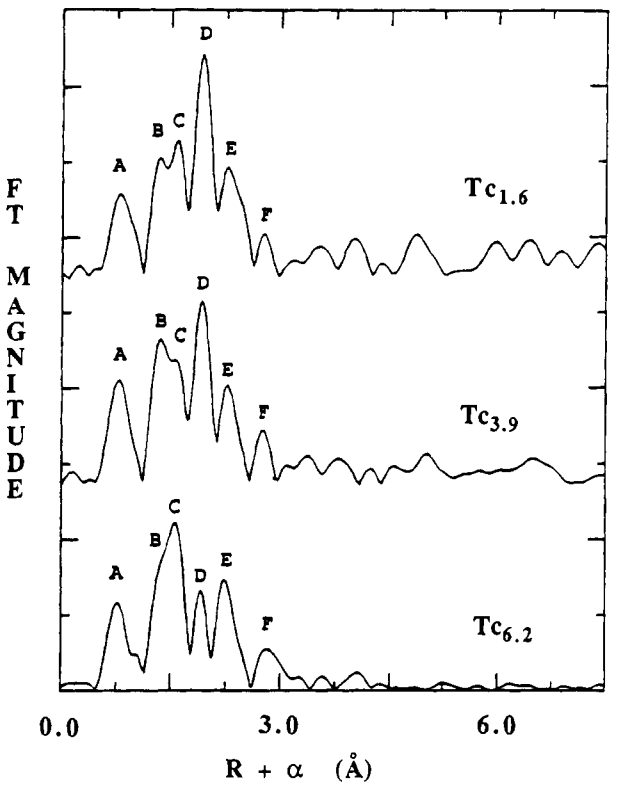

Figure 6. Pseudo-radial distribution functions calculated by Fourier transformation of the normalized Tc K-edge EXAFS data for three Tc_x-MT (x = 1.6, 3.9, 6.2) samples.

theoretical[31] or experimental scattering parameters. The results of this analysis are found in Table 3. The $Tc_{1.6}$-MT EXAFS data are considered first, followed by extension to the samples with higher Tc content.

The first peak, A, is found at the unreasonably close distance of 0.8 Å $R+\alpha$. Further, its filtered back-transformed envelope maximizes in the 8.25–13.0 $Å^{-1}$ region, where the raw EXAFS

(31) Teo, B.-K.; Lee, P. A. *J. Am. Chem. Soc.* **1979**, *101*, 2815–2832.

Table 3. Fitting of Tc_x-Metallothionein EXAFS Data

shell	fit	atom	coordn no.[a]	bond length, Å[a]	$\Delta E(0)$, eV	fit value[c]
			$Tc_{1.6}$-MT			
BC	theor	=O	0.56	1.64	6.5	
		−O	2.51	2.04	2.8	0.45
BC	theor	=O	1.00[b]	1.65[b]	0.0[b]	
		−O	2.56	2.05	−0.2	0.55
BC	empir	=O	0.99	1.70	−23.3	
		−O	1.62	2.03	23.9	0.28
BC	empir	=O	1.00[b]	1.65[b]	0.0[b]	
		−O	1.66	2.03	13.4	0.64
D	empir	−S	1.61	2.32	−6.3	0.39
E	theor	−Tc	0.61	2.60	−3.6	0.37
F	theor	−Zn	0.32	3.11	−2.0	0.09
			$Tc_{3.9}$-MT			
BC	theor	=O	0.71	1.65	−1.9	
		−O	2.53	2.02	0.0	0.51
BC	theor	=O	1.00[b]	1.65[b]	0.0[b]	
		−O	2.65	2.02	0.2	0.56
BC	empir	=O	1.15	1.69	−25.6	
		−O	1.24	2.02	19.4	0.19
BC	empir	=O	1.00[b]	1.65[b]	0.0[b]	
		−O	1.55	2.01	10.4	0.71
D	empir	−S	1.28	2.31	−8.5	0.32
E	theor	−Tc	0.51	2.58	1.5	0.18
F	theor	−Zn	0.42	3.08	−2.8	0.10
			$Tc_{6.2}$-MT			
BC	theor	=O	0.59	1.67	−10.7	
		−O	2.93	2.01	−3.5	0.31
BC	theor	=O	1.00[b]	1.65[b]	0.0[b]	
		−O	3.11	2.01	−1.3	0.43
BC	empir	=O	0.98	1.70	−32.6	
		−O	1.75	2.01	12.8	0.09
BC	empir	=O	1.00[b]	1.65[b]	0.0[b]	
		−O	2.18	2.00	7.7	0.75
D	empir	−S	0.54	2.30	−10.9	0.19
E	theor	−Tc	0.61	2.56	4.6	0.19
F	theor	−Zn	0.44	3.15	−15.3	0.12

[a] Error estimates: coordination number, ±30%; bond length, ±0.02 Å. [b] Value held constant throughout the calculation. [c] Goodness of fit = $[\sum_{pts}(k^3(EXAFS_{obs} - EXAFS_{calc})^2/N_{pts})]^{1/2}$.

spectrum (Figure 5) exhibits significant noise and little structure. This suggests peak A is an artifact which can be attributed to the residual background;[32] it is not considered further.

Peaks B and C, which arise from backscattering by first shell ligand atoms, are not resolved and were filtered together and analyzed simultaneously using several models to evaluate reasonable possibilities. The amplitude of the envelope of the filtered, back-transformed EXAFS data for these two peaks maximizes at ~7.0 $Å^{-1}$, suggesting low-Z backscattering atoms. The 940 cm^{-1} Tc=O band in the Raman spectrum suggests that peak B originates from backscattering by a tightly bound oxo ligand, and the 405 nm Cys-to-Tc(V) CT band in the absorption spectrum suggests that peak C might be due to S backscattering. Initially, a two shell model, consisting of theoretical phase and amplitude functions for O backscattering and empirical phase and amplitude functions, extracted from analysis of EXAFS data on $NaTcO(edt)_2$, for S backscattering, was used to fit the filtered back-transformed data. Bond length, coordination number and $\Delta E(0)$ (energy at which $k = 0$) for both shells were refined simultaneously but the calculation quickly diverged. Fixing a single Tc−O bond length at 1.65 Å, a value consistent with a number of TcO^{3+} complexes,[13,14,18,22] and refining the Tc−S parameters led to convergence but a poor fit, consisting of only a single S backscatterer at the unreasonably short distance of 2.1 Å. Subsequently, a two shell model, consisting only of O backscattering and using either theoretical or empirical functions, the latter extracted from analysis of EXAFS data on $NaTcO_4$, was used to fit the filtered EXAFS data for peaks B and C (Table 3); duplicate fits were performed holding the short Tc−O parameters fixed. The best fit (lowest goodness of fit value) was obtained using the empirical parameters and allowing both shells to refine simultaneously. It shows a single oxo ligand at 1.70 Å and 1−2 O (or N) first shell atoms at an average distance of 2.03 Å. All four fits, however, give a relatively consistent set of values, with those using the theoretical parameters suggesting a somewhat higher number of O/N scatterers. These results are consistent with crystallographic data for many TcO^{3+} complexes[22] and indicate ligands other than Cys thiolates for Tc bound to MT.

Peak D, which occurs at 1.92 Å $R+\alpha$ in the FT-EXAFS spectrum, was filtered and back-transformed. The envelope amplitude maximizes at 8.5 $Å^{-1}$, which is close to the maximum of the filtered back-transformed EXAFS data for the Tc−S peak of $NaTcO(edt)_2$. Using empirical S backscattering phase and amplitude functions, obtained from analysis of EXAFS data on $NaTcO(edt)_2$, the bond length, coordination number and $\Delta E(0)$ were refined simultaneously for peak D; the fit converged to indicate this peak represents 1−2 S (or Cl) backscatterers at a Tc−S(Cl) bond length of 2.32 Å, consistent with several TcO^{3+} thiolate complexes.[13,14,18]

Peak E is substantially higher than the background and its filtered back-transformed envelope maximizes at the high k value of 12.5 $Å^{-1}$. This is similar to the value found for Tc backscattering in an analysis of EXAFS data on $(TcO)_2(edt)_3$. Due to the clustering nature of metal binding to MT, short Tc−Zn or Tc−Tc distances in these samples were not unexpected. Theoretical phase and amplitude functions for both Tc and Zn scattering were fitted to the filtered EXAFS data for peak E. Similar results were obtained for both metals; however, the Tc backscattering gave a somewhat better fit for 0−1 Tc at 2.60 Å.

The final noticeable peak in the FT-EXAFS data, peak F, is not above the background for the $Tc_{1.6}$-MT sample but is slightly above the background for the $Tc_{3.9}$-MT and $Tc_{6.2}$-MT samples (Figure 6). While this peak has low intensity and is difficult to fit, the filtered back-transformed EXAFS envelope does maximize toward higher k value (for $Tc_{6.2}$-MT it maximizes at 8.8 $Å^{-1}$), suggesting it correlates with higher Z (S, Cl, Tc or Zn) backscattering. Although second shell atoms of the Tc ligands likely contribute to this peak, fitting the peak F filtered back-transformed EXAFS data with the same Tc or Zn functions used to fit peak E suggests that 0−1 Tc or Zn scatterers at 3.11 Å are the dominant contribution to this peak.

The EXAFS data for the other two samples were fit as described above and comparison of the fits (Table 3) indicates changes in the average TcO^{3+} coordination with increasing levels of Tc bound to MT. The best fits for peaks B and C give one oxo ligand at 1.69 ± 0.02 Å, consistent with structurally characterized TcO^{3+} complexes, and approximately two O or N donor ligands at 2.02 ± 0.02 Å for all three samples. Fitting peak D for S backscattering shows 1−2 S (or Cl) ligands at 2.31 ± 0.03 Å for low levels of Tc and a *decrease* in the average number of S backscatterers upon higher Tc loading. Peak E can be fit to a relatively constant ~0.5 Tc or Zn backscattering at 2.58 ± 0.04 Å during all stages of TcO^{3+} binding. Finally, peak F, though probably comprised of contributions from more than one type of scatterer, can be fit to ~0.5 Zn or Tc backscattering at 3.11 ± 0.06 Å in all samples.

The set of best fit parameters (Table 3) for the five shells (B−F) were used to calculate EXAFS spectra for the three

(32) Teo, B.-K. *EXAFS: Basic Principles and Data Analysis*; Springer-Verlag: Berlin, 1986.

samples. These calculated spectra are superimposed on the experimental spectra in Figure 5 and are found to reproduce the general features of the Tc K-edge EXAFS data at all levels of Tc loading of MT.

Discussion

The objective of this study was to provide detailed insight about technetium coordination to metallothionein for nuclear medicine applications of ^{99m}Tc. Tc_x-MT (x = 1.6, 3.9, 6.2) samples were prepared by the transchelation reaction of $TcO(GH)_2^-$ with Zn_7-MT, which is particularly attractive for the preparation of ^{99m}Tc-labeled MT–antibody complexes since (1) TcO^{3+} is kinetically inert and has a reasonably high affinity for thiolate ligands,[13,14,18] (2) $^{99m}TcO(GH)_2^-$ can be prepared readily in clinical settings,[33] (3) Zn_7-MT is a stable well-characterized form of the protein,[4] and (4) $^{99}TcO^{3+}$ has been shown to bind relatively quickly and very tightly to Zn_7-MT.[12] Thus, the samples studied here are directly relevant to potential clinical applications of this chemistry.

TcO^{3+} Coordination to MT. Because of the high Tc/MT ratio for some of these Tc,Zn-MT samples, it was important to determine initially if there was heterogeneity in the Tc coordination and/or oxidation state. The increase in intensity of the 940 cm^{-1} Raman band with increasing Tc stoichiometry indicates that each Tc has an oxo ligand and is in the same high oxidation state. There are no Raman data to suggest formation of the *trans* dioxo ion, O=Tc=O$^+$ (symmetric vibration at ~800 cm^{-1}),[34] and analysis of the EXAFS data indicates only a single oxo ligand. Vibrational data indicative of μ-oxo ligation, Tc–O–Tc (symmetric vibration in the 650–700 cm^{-1} region),[35] are also not observed, and there is no evidence from the EXAFS data for a 1.90–1.92 Å Tc–O(bridge) bond length.[35] Although Tc(V) chemistry is dominated by square pyramidal coordination of the TcO^{3+} ion, our Raman, ligand field and EXAFS data can not exclude the possibility of a sixth ligand *trans* to the oxo in these samples. However, a Tc=O bond length of 1.70 Å, as found by analysis of the Tc,Zn-MT EXAFS data, is in better agreement with five-coordinate TcO^{3+}. Also, there is no evidence for a change in the Tc coordination number with higher Tc stoichiometries, as a 40–80 cm^{-1} shift of the Tc=O vibration to lower energy should be associated with addition of a sixth ligand.[36] Finally, there is no Raman evidence for cysteine oxidation[37] (*RS-SR* symmetric vibration in the 500–550 cm^{-1} region), and thus Tc reduction during transchelation. Therefore, in these samples each Tc is most likely bound to MT as the TcO^{3+} ion in a similar square pyramidal coordination.

While the most simple model for TcO^{3+} binding to Zn_7-MT would involve isomorphous metal replacement, the different coordination preferences and metal–ligand bond strengths of the two metal ions probably make this process more complex. However, EXAFS evidence for O/N donor ligands, in addition to the tightly bound oxo of TcO^{3+}, was unexpected. While there may be a 1:1 replacement of Zn(II), the TcO^{3+} ion does not recruit four equatorial Cys thiolate ligands. Although ligands other than Cys have been reported for Au(I) in Au_{20}-MT[9] and for Cd(II) in $Ag_{17}Cd_2$-MT[29c] and $Cd_{13}(P_i)_2$-MT (P_i = phosphate) formed at elevated temperatures,[38] this is the first report of non-Cys ligands for a metal ion bound to MT under standard conditions and at low metal ion stoichiometries.

The $^1E \leftarrow {}^1A_1$ ligand field transition of square pyramidal TcO^{3+} complexes is observed typically as a weak band ($\epsilon \approx 100$ M^{-1} cm^{-1}) or shoulder in the 500–600 nm region of the absorption spectrum (Table 2) and its energy reflects the overall ligand field strength. This absorption band is found at ~570 nm for these Tc,Zn-MT samples. A recently prepared series of TcO^{3+} complexes[39] have amide–thiolate–thioether chelating ligands, which provide a somewhat stronger ligand field ($^1E \leftarrow {}^1A_1$ at 512 ± 4 nm) than that found for TcO^{3+} bound to MT. However, absorption data remarkably similar to that of Tc,Zn-MT, including a $^1E \leftarrow {}^1A_1$ transition at 564 nm, are reported for the complex $TcO(pen^{2-})(pen^-)$ (pen = D-penicillamine), which has bis(thiolate), bis(amine) equatorial ligation and a weakly bound axial carboxylate.[40]

The non-Cys ligands of TcO^{3+} may include the 12 serines and threoneins or the 7 lysines located adjacent to the 20 cysteines in rabbit liver MT-1, or hydroxide (or water). The high affinity of MT for TcO^{3+} suggests that more protein ligands than two Cys are involved in binding this metal ion. Alternatively, glucoheptonate may be retained as a ligand during TcO^{3+} binding to the protein, analogous to the retention of thiomalate (Tm) in the transchelation binding of AuTm to native Cd,Zn-MT.[9] A precedent for GH as the non-Cys ligands of TcO^{3+} is found in the retention of a GH ligand from $TcO(GH)_2^-$ or an ethylene glycol (Eg) ligand from $TcO(Eg)_2^-$ in the synthesis of TcO^{3+} complexes in aqueous solution.[41] The 2.02 ± 0.02 Å Tc–O/N bond length, determined by analysis of the Tc,Zn-MT EXAFS data, appears to be more consistent with O donor ligands;[22] however, the $Tc_{6.2}$-MT sample exhibits a weak Raman band at 475 cm^{-1} (data not shown), which may be a Tc–N stretching mode.[40,42,43] The presence of non-Cys ligands may be a consequence of the "hardness" of this metal ion.

Another unexpected feature of these samples is the EXAFS evidence for Tc or Zn backscattering at the relatively short distance of 2.6 Å. While the shortest metal–metal distance in native MT is 3.7 Å,[8] Cu(I)–Cu(I) distances of 2.7 Å have been reported in EXAFS studies of fungal,[10b] yeast[10c] and mammalian[30] Cu-MT. Numerous dinuclear Tc complexes with Tc–Tc distances ranging from 2.13 to 7.17 Å have been structurally characterized,[22] although few of these involve higher oxidation states and only two have the TcO^{3+} core.[14,44] While the dinuclear complex $(TcO)_2(edt)_3$ with bridging thiolates appears to be relevant to TcO^{3+} binding to MT, the 3.65 Å Tc–Tc distance[14b] in this compound is considerably longer than that found by EXAFS for Tc,Zn-MT; possibly the shorter separation

(33) de Kieviet, W. *J. Nucl. Med.* **1981**, *22*, 703–709.
(34) Zuckman, S. A.; Freeman, G. M.; Troutner, D. E.; Volkert, W. A.; Holmes, R. A.; van der Veen, D. G.; Barefield, E. K. *Inorg. Chem.* **1981**, *20*, 2386–2389.
(35) (a) Bandoli, G.; Nicolini, M.; Mazzi, U.; Refosco, F. *J. Chem Soc., Dalton Trans.* **1984**, 2505–2510. (b) Pillai, M. R. A.; John, C. S.; Lo, J. M.; Schlemper, E. O.; Troutner, D. E. *Inorg. Chem.* **1990**, *29*, 1850–1856.
(36) (a) Thomas, R. W.; Heeg, M. J.; Elder, R. C.; Deutsch, E. *Inorg. Chem.* **1985**, *24*, 1472–1477. (b) Tisato, F.; Refosco, F.; Mazzi, U.; Bandoli, G.; Nicolini, M. *J. Chem Soc., Dalton Trans.* **1987**, 1693–1699.
(37) Oxidized Cys has a weak absorption band (ϵ = 300 M^{-1} cm^{-1}) and CD intensity at 250 nm, but we are unable to tell if this contributes to the broad positive 240–270 nm CD band (Figure 2), assigned as a thiolate-to-Tc(V) CT transition.
(38) Palumma, P.; Zerbe, O.; Vasák, M. *Biochemistry* **1993**, *32*, 2874–2879.
(39) Bryson, N.; Dewan, J. C.; Lister-James, J.; Jones, A. G.; Davison, A. *Inorg. Chem.* **1988**, *27*, 2154–2161.
(40) Franklin, K. J.; Howard-Lock, H. E.; Lock, C. J. L. *Inorg. Chem.* **1982**, *21*, 1941–1946.
(41) Linder, K. E.; Davison, A.; Jones, A. G. in *Technetium in Chemistry and Nuclear Medicine 2*; Nicolini, M., Bandoli, G., Mazzi, U., Eds.; Raven: New York, 1986; pp 43–44.
(42) Davison, A.; Pearlstein, R. M.; Mabrouk, P. A.; Jones, A. G.; Morelock, M. M. In *Technetium in Chemistry and Nuclear Medicine 2*; Nicolini, M., Bandoli, G., Mazzi, U., Eds.; Raven: New York, 1986; pp 25–27.
(43) Bandoli, G.; Gerber, T. I. A. *Inorg. Chim. Acta* **1987**, *126*, 205–208.
(44) Bryson, N.; Brenner, D.; Lister-James, J.; Jones, A. G.; Dewan, J. C.; Davison, A. *Inorg. Chem.* **1989**, *28*, 3825–3828.

is forced by the protein structure. Recently a mixed-valent dinuclear Tc(V)−Tc(IV) complex with catecholate ligands and bridging phenylhydrazines was reported to have a 2.61 Å Tc−Tc distance.[45] Model complexes, thus, provide some precedent for the 2.6 Å Tc−Tc(Zn) separation found in Tc,Zn-MT but do not support Cys bridging of this metal−metal distance.

Vibrational, optical and EXAFS data all indicate there is no *major* change in the average TcO^{3+} coordination as the Tc content increases. Among these data, the constant energy of the 405 nm CT transition is particularly informative. It is known that the energies of charge transfer transitions are perturbed by bridging coordination in homodinuclear complexes,[46] and the presence of metal clusters and bridging Cys ligands in MT has been associated with a red shift of Cys-to-metal CT bands.[47] Of particular relevance, Davison and co-workers have shown that $(TcO)_2(edt)_3$, with bridging thiolates, has a lower energy thiolate-to-Tc(V) CT transition than that of $TcO(edt)_2^-$.[14a] Thus, since this CT transition has the same energy (405 nm) for all three Tc,Zn-MT samples, either there is only terminal Cys coordination to TcO^{3+} or there is the same degree of Tc−Cys−Tc bridging at all Tc stoichiometries. While the former may seem unlikely for MT samples with high Tc stoichiometries, by comparison to the terminal and bridging Tc−S bond lengths in $(TcO)_2(edt)_3$,[14b] the constant 2.31 ± 0.02 Å Tc−S bond length in Tc,Zn−MT supports only terminal Tc−S bonding. The spectral data on these samples, however, do not rule out Tc−Cys−Zn bridging.

Transchelation Binding of TcO^{3+} to Zn_7-MT. Metal binding to MT by transchelation has been studied for (1) Cd(II),[48] Hg(II),[49] Ag(I),[50] Cu(I)[51] and Pt(II)[11c] binding to Zn_7-MT, (2) Hg(II),[52] Cu(I),[51] and Pt(II)[11a] binding to Cd_7-MT, and (3) Au(I)[9] and Pt(II)[11a] binding to native Cd,Zn-MT, and evidence supporting either a random or a domain-specific process has been reported. In this study, characterization of the TcO^{3+} coordination in Tc_x-MT samples with low ($x = 1.6$), medium ($x = 3.9$) and high ($x = 6.2$) levels of Tc loading provides some new insight about transchelation binding of TcO^{3+} to Zn_7-MT.

While the similar TcO^{3+} coordination geometry and the constant 2.6 and 3.1 Å metal (Tc or Zn) scattering in all Tc,Zn-MT samples would be consistent with a cooperative binding process, the decrease in the number of S(Cl) scatterers and the negligible increase in the integrated intensity of the 405 nm thiolate-to-Tc(V) CT band between the $Tc_{3.9}$-MT and the $Tc_{6.2}$-MT samples clearly is not. The constant energy of the 405 nm CT band and the identical 2.31 ± 0.02 Å Tc−S bond length in all three samples together indicate that TcO^{3+} binds without any bridging Cys; this, however, would be consistent either with random binding to the whole protein or with binding to only one domain, since up to ~5 TcO^{3+} ions, each with only two terminal Cys ligands, could bind to either domain. Finally, previously reported[12] results of a 2,2′-dithiodipyridine (DTDP) titration of free thiols in Tc,Zn-MT samples indicate that only 10 ± 1 of the Cys are involved in TcO^{3+} binding in samples with ~2 to ~6 mol equiv Tc,[53] and the sigmoidal shape of these titration data contrasts dramatically with the steady decrease in free thiols reported for an analogous 5,5′-dithiobis(2-nitrobenzoic acid) (DTNB) titration of Pt_x-MT ($x = 0-7$) samples, where Pt(II) is randomly bound to MT;[11b] this argues against a random process but suggests a domain-specific binding of TcO^{3+} to Zn_7-MT. While it has been shown that TcO^{3+} binds with similar kinetics to either domain,[12] thermodynamics may favor coordination to one domain of Zn_7-MT, as found for both unipositive and dipositive metal ions.[4,6]

Although definitive insight about transchelation binding of TcO^{3+} to Zn_7-MT has not been obtained, it is clear that either there are severe restrictions on the availability (accessibility) of the MT cysteines or some O/N donor ligands from the protein (or possibly glucoheptonate) are not displaced by the Cys thiolates. The unique ligand set, consisting of ~2 O/N donor ligands, for TcO^{3+} bound to MT indicates that transchelation does not involve simple substitution of tetrathiolate square pyramidal TcO^{3+} for tetrathiolate T_d Zn(II). This may be due to structural restrictions imposed by the protein and/or the thermodynamics of TcO^{3+} bonding to MT.

Acknowledgment. We thank David Dooley for use of the Amherst College Raman equipment and technical assistance, John Winn for assistance with the band shape analysis, and Jie Yuan for preparation of the calculated EXAFS spectra. We gratefully acknowledge Edward Deutsch for valuable discussions, Karen Wetterhahn for insightful comments, and Thomas Tulip for encouragement in this study. EXAFS studies were performed at the Stanford Synchrotron Radiation Laboratory supported by DOE and used biotechnology facilities provided by NIH. R.C.E. thanks the NIH for support (Grant No. GM35404) and W.B.J. thanks the University of Cincinnati for a Lowenstein-Schubert-Twitchell Fellowship.

(45) Abrams, M. J.; Larsen, S. K.; Zubieta, J. *Inorg. Chem.* **1991**, *30*, 2031−2035.
(46) Desjardins, S. R.; Wilcox, D. E.; Musselman, R. L.; Solomon, E. I. *Inorg. Chem.* **1987**, *26*, 288−300.
(47) (a) Vasák, M.; Kägi, J. H. R. *Proc. Natl. Acad. Sci. U.S.A.* **1981**, *78*, 6709−6713. (b) Good, M.; Vasák, M. *Biochemistry* **1986**, *25*, 8353−8356. (c) Wilner, H.; Vasák, M.; Kägi, J. H. R. *Biochemistry* **1987**, *26*, 6287−6292.
(48) (a) Nettesheim, D. G.; Engeseth, H. R.; Otvos, J. D. *Biochemistry* **1985**, *24*, 6744−6751. (b) Stillman, M. J.; Cai, W.; Zelazowski, A. J. *J. Biol. Chem.* **1987**, *262*, 4538−4548.
(49) Lu, W.; Zelazowski, A. J.; Stillman, M. J. *Inorg. Chem.* **1993**, *32*, 919−926.
(50) Zelazowski, A. J.; Stillman, M. J. *Inorg. Chem.* **1992**, *31*, 3363−3370.
(51) Stillman, M. J.; Law, A. Y. C.; Cai, W.; Zelazowski, A. J. In ref 4b, pp 203−211.
(52) Johnson, B. A.; Armitage, I. M. *Inorg. Chem.* **1987**, *26*, 3139−3144.

(53) Figure 3 of ref 12 indicates the following numbers of Cys are inaccessible to DTDP when the indicated Tc equivalents are bound to MT: Tc_1, 6; Tc_2, 9; Tc_3, 10; Tc_4, 10; Tc_5, 10; Tc_6, 11; $Tc_{6.8}$, 15.